

INVESTIGATING THE IMPACT OF TB OR COVID-19 INFECTIONS ON A POPULATION SUFFERING FROM TB/COVID-19 COINFECTION

Abstract

The discovery that the spread of tuberculosis reduced significantly in the last two years has been associated with the preventive measures placed to combat the spread of COVID-19. This shows a strong correlation between the spread of COVID-19 and tuberculosis in any population. It is worth noting that tuberculosis and COVID-19 are among the leading most deadly diseases in the world today. The correlation in their spread also leaves us to believe that the spread of one can enhance the spread of the other. Hence, we propose the situation where a population is co-infected with the two diseases. The mathematical model is formulated using conservative laws and the resulting model analysed. The stability of the co-infection is analysed and the non-negativity conditions for the solution is established. It is found that tuberculosis sub-population reaches the highest capacity when the recruitment into the COVID-19 subpopulation is the lowest while the COVID-19 sub-population is attained when the rate of recruitment into the COVID-19 subpopulation is the highest.

Keywords: COVID-19, Tuberculosis, Coinfection, epidemiology, mathematical modelling

Nomenclature

Symbol	Meaning	Symbol	Meaning
S	Susceptible compartment	T	Tuberculosis infected compartment
C	COVID-19 infected compartment	I	co-infected compartment
Λ	influx rate into the susceptible population	R	recovered compartment
α_1	recruitment rate into C	p_1	proportion of E migrating into C
α_2	recruitment rate into T	p_2	proportion of E migrating into T
r_1	recovery rate of C	β_1	rate at which members of C get co-infected with tuberculosis
r_2	recovery rate of T	β_2	rate at which members of T get co-infected with COVID-19
r_3	recovery rate of I	ϵ	rate at which R losses its immunity
d_1	COVID-19-induced death rate	μ	natural death rate
d_2	tuberculosis-induced death rate		

1 Background Information

COVID-19, a short form of coronavirus disease that spiked into a pandemic in 2019, is a disease caused by SARS-CoV-2. It originated from Wuhan, China. The coronavirus is a virus family that originated in animals but has now been discovered to infect humans with respiratory diseases. They were not considered fatal until COVID-19 evolved, which has claimed the lives of over 6 million people globally. Although the first instance was reported in Wuhan, China, it is still unknown how the sickness was transmitted to humans. However, it is thought that the disease originated in bats, wolf pulps, or (Toit, 2020). Ever since the virus into one human from an unknown origin, it has since spread from human to human. The spread happens by contaminated droplets when infected people sneeze, or cough (Seifirad, 2020; Bada *et al.*, 2021). Symptoms of infection include high fever, breath shortness, cough, and running nose. Symptoms begin to appear within the fourteen days from the day of infection (Horowitz and Freeman, 2020; Kumar Raghav and Mohanty, 2020). Emergence of COVID-19 in 2019 has brought about a paradigm shift in many facets of human endeavours. The mortality rate was very high and it became the most deadly disease in 2020. It is also important to note that in spite of the enormous resources directed into research on COVID-19, little progress has been made to unravel the mysteries surrounding the disease. The rapid evolution and mutation of COVID-19 makes it difficult for scientists to come up with a cure. In the least, vaccines have been developed to prevent infection with COVID-19 (Li *et al.*, 2021). Tuberculosis on the other hand has been around for decades but it has not been considered as a global pandemic despite claiming more lives than 90% of other infectious diseases. Tuberculosis has been given less attention than it deserves in this past decade and Bates and Stead (1993) had advocated that tuberculosis should be named a global epidemic. Bates and Stead (1993) pointed out that the duration of tuberculosis in a population is an important factor in properly understanding the trend in the population.

Tuberculosis is bacterial infection caused by the mycobacterium tuberculosis. It is an infection of the lungs, kidney and the spine that is transmitted via droplets from infected individuals. The infection is in two phases; the latent phase and the active phase (Nainggolan *et al.*, 2013). The latent phase of the tuberculosis infection is not harmful to the body and produces no symptom but the active phase becomes a major sickness after months or years of infection (Okuonghae and Ikhimwin, 2016; Kabunga *et al.*, 2020).

COVID-19 disease presence in an individual makes the individual vulnerable to tuberculosis while the presence of tuberculosis makes the individual vulnerable to COVID-19. Hence, one of the diseases can come as secondary infection when an individual is infected with the other. COVID-19 has claimed the lives of around 6.32 million human beings globally since 2019 and it is classified as the most deadly infectious disease globally. Tuberculosis is the next in line, killing over 1.5 million individuals in 2020. This shows the threat posed on an individual if they are co-infected with both COVID-19 and tuberculosis (CDC, 2020). Equipped with these pieces of information, it becomes very pertinent to examine the flow of COVID-19/tuberculosis co-infection in a population. A mathematical model to examine the dynamics of COVID-19/tuberculosis co-infection in a population is investigated in this study. The qualitative analysis of the model shall be carried out to establish the conditions for the existence and uniqueness of solution. By simulating the model for various parameter values, the variation of COVID-19/tuberculosis co-infection in a given population is investigated.

Mathematical modelling provides scientists with a very economical approach to study the trend of an epidemic. The disease and its trend can be studied before it hits the population and vital recommendations can be made even before the disease hits the population (Oke & Bada, 2019; Bada *et al.*, 2021; Kimulu *et al.*, 2022a; Kimulu *et al.*, 2022b; Zafar *et al.*, 2022; Ndendya *et al.*, 2024; Oswald *et al.*, 2024). In the case of COVID-19, scientists were quick to formulate mathematical models for the transmission of the disease (Kimulu *et al.*, 2023; Okundalaye *et al.*, 2022; Paul *et al.*, 2021; Paul *et al.*, 2023; Paul *et al.*, 2024). Aldila *et al.* (2020) proposed a mathematical model for investigating effects of social distancing as a measure for controlling the COVID-19 spread, with emphasis on prompt testing. Annas *et al.* (2020) adopted mathematical model for studying the spread of COVID-19 in Indonesia. Oke *et al.* (2021) studied the possibility of re-infection, relapse or recurrence of COVID-19 in recovered individuals. Wangari *et al.* (2021) included the hospitalised compartment, contact tracing, and testing in large groups on the impact of reinfection of COVID-19 in the mathematical modelling of trend of COVID-19 in Kenya. The mathematical model formulated by Ayinla *et al.* (2021) was used to predict tuberculosis epidemic and they found that lowering the rate of vaccination gives tuberculosis a higher chance of persisting in any population. Recently, Mekonen *et al.* (2022) had considered the possibility of co-infection of tuberculosis and COVID-19. The study proposed an 8-compartment mathematical model in which the recovered compartment is considered as an absorbing state. This study aims at modifying the work of Mekonen *et al.* (2022). It is interesting to observe that some of the 8 compartments proposed by Mekonen *et al.* (2022) can be merged into a single compartments. Also, Mekonen *et al.* (2022) had considered the recovered compartment

as an absorbent state, whereas it has been recorded by Oke *et al.* (2021) that relapse and reinfection are possible. Hence, this study proposes a 5-compartment mathematical model to investigate the co-infection of COVID-19 and tuberculosis dynamics.

The social nature of human beings makes the human population vulnerable to rapid spread of infectious diseases. COVID-19 and tuberculosis are the two leading most deadly infectious diseases. It is alarming to observe that over 2 million deaths were related to COVID-19 in 2020 and over 1.5 million deaths were related to tuberculosis in 2020. This indicates the possible fatality embedded in the existence of the co-infection of both diseases in a population. Hence, this research focuses on COVID-19/tuberculosis co-infection dynamics in a population. The preventive measures against COVID-19 are also good measures to achieve reduction in the transmission of tuberculosis in a population. Meanwhile, if the two diseases should hit a certain population at the same time, it appears the population will be badly affected. In lieu of this, this study considers the trend when there is COVID-19/tuberculosis co-infection in a population. The simulations from this study shall provide a trend to expect in any case the a population is hit by the COVID-19/tuberculosis co-infection. In addition, the outcome of this research shall provide a significance for further research.

2 Methodology

An SCTIR mathematical model that considers the dynamics of the individuals who get co-infected with both tuberculosis and COVID-19 is formulated in this section. The population is compartmentalised into five groups of susceptible group S , COVID-19 infected group C , Tuberculosis infected group T , COVID-19 and tuberculosis co-infected group I , and Recovered group R . The susceptible group is the part of the population who possess a chance of contracting either COVID-19 or tuberculosis. Individuals who have COVID-19 only are classed into the COVID-19 infected group, individuals who are infected with tuberculosis only are classed into the tuberculosis group and individuals who have both COVID-19 and tuberculosis are classed in the Infected group. The recovered class consists of all individuals who have been cured of any of the diseases. The model is formulated built on the following assumptions;

- (i) Every member of the population gives birth to healthy children (i.e. without tuberculosis or COVID-19).
- (ii) Tuberculosis and COVID-19 are transmitted by interaction with infected individuals.
- (iii) Individuals infected with either tuberculosis or COVID-19 or both either recover or die.
- (iv) Individuals from each compartment can die a natural death.

In subsequent sections, the reproduction numbers for the co-infection are obtained using the next generation matrix (NGM) for the mathematical model. The non-negativity conditions are established for the model and the stability of the equilibrium points are also obtained.

2.1 Modal Formulation

In this model, we assume that individuals are born into the population without tuberculosis or COVID-19 and at the rate Λ . An individual is considered susceptible if they are not infected with COVID-19 or TB. Susceptible individuals get COVID-19 at the rate α_1 when they interact with individuals carrying COVID-19. Also, a susceptible individual gets infected with tuberculosis at the rate α_2 when they interact with individuals who are already infected with tuberculosis. Individuals infected with COVID-19 or TB remain in thier category unless they there is an interaction between the classes. The COVID-19 infected individuals who interacted with tuberculosis patients also get tuberculosis at the rate of β_1 while tuberculosis-infected individuals who interacted with COVID-19-infected get also get COVID-19 at the rate of β_2 . The rates at which individuals infected with COVID-19 only, tuberculosis only, and co-infected with both diseases recover from their infections are r_1, r_2, r_3 respectively. Individuals from the population

die natural death at the rate μ , COVID-19 induced deaths occur at the rate d_1 , tuberculosis-induced deaths occur at the rate d_2 . Figure 3.1 shows the pictorial representation of the model.

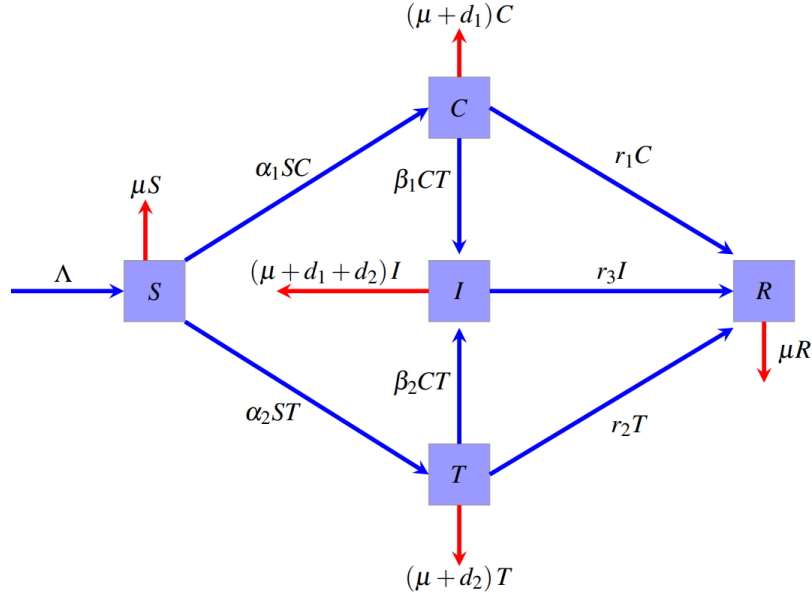


Figure 2.1: Spread configuration

The dynamics of co-infection of both COVID-19 and tuberculosis described so far is modelled into the system of equations;

$$\frac{dS}{dt} = \Lambda - \mu S - \alpha_1 SC - \alpha_2 ST, \quad (2.1)$$

$$\frac{dC}{dt} = \alpha_1 SC - \beta_1 CT - (\mu + d_1)C - r_1 C, \quad (2.2)$$

$$\frac{dT}{dt} = \alpha_2 ST - \beta_2 CT - (\mu + d_2)T - r_2 T, \quad (2.3)$$

$$\frac{dI}{dt} = \beta_1 CT + \beta_2 CT - (\mu + d_1 + d_2)I - r_3 I, \quad (2.4)$$

$$\frac{dR}{dt} = r_1 C + r_2 T + r_3 I - \mu R. \quad (2.5)$$

with the following conditions;

$$0 \leq \mu, \alpha_1, \alpha_2, \beta_1, \beta_2, d_1, d_2, r_1, r_2, r_3, \epsilon \leq 1,$$

and the entire population $N(t)$ at any time t is given by

$$N(t) = S(t) + C(t) + T(t) + I(t) + R(t). \quad (2.6)$$

2.2 Nonegativity and boundedness

Summing up equations (3.2.1) - (3.2.5), we have

$$\frac{d}{dt}(S + C + T + I + R) = \Lambda - \mu(S + C + T + I + R) - d_1C - d_2T - (d_1 + d_2)I. \quad (2.7)$$

Using equation (3.2.6), we have

$$\frac{dN}{dt} = \Lambda - \mu N - d_1C - d_2T - (d_1 + d_2)I \leq \Lambda - \mu N. \quad (2.8)$$

Hence, by separating the variables, the equation is solved to get

$$N \leq \frac{\Lambda}{\mu} - \left(\frac{\Lambda}{\mu} - N(0) \right) \exp(-\mu t), \quad (2.9)$$

where $N(0)$ is the initial population. As $t \rightarrow \infty$,

$$N \rightarrow \frac{\Lambda}{\mu}. \quad (2.10)$$

Hence, the problem is epidemiologically feasible and the solution can be sought in the region

$$\mathcal{R} = \left\{ (S, C, T, I, R) : S + C + T + I + R \leq \frac{\Lambda}{\mu} \right\}. \quad (2.11)$$

2.3 Qualitative Analysis of the Model

2.3.1 Equilibrium Points

The first step in the qualitative analysis is to obtain the equilibrium points. This is done by setting the right hand side of each of the equations (3.2.1) - (3.2.3) to zero as follows;

$$\Lambda - \mu S - \alpha_1 SC - \alpha_2 ST = 0, \quad (2.12)$$

$$\alpha_1 SC - \beta_1 CT - (\mu + d_1)C - r_1 C = 0, \quad (2.13)$$

$$\alpha_2 ST - \beta_2 CT - (\mu + d_2)T - r_2 T = 0, \quad (2.14)$$

$$\beta_1 CT + \beta_2 CT - (\mu + d_1 + d_2)I - r_3 I = 0, \quad (2.15)$$

$$r_1 C + r_2 T + r_3 I - \mu R = 0. \quad (2.16)$$

The disease free equilibrium (DFE) is the equilibrium obtained in the absence of diseases in the population, that is, $C = T = I = 0$. Thus, we have the DFE E_0 as $E_0 = (S_0, C_0, T_0, I_0, R_0) = \left(\frac{\Lambda}{\mu}, 0, 0, 0 \right)$.

The endemic equilibrium point (EEP) is obtained as $(S^*, C^*, T^*, I^*, R^*)$, where

$$S^* = \frac{\Lambda}{\mu + \alpha_1 C^* + \alpha_2 T^*}, \quad R^* = \frac{r_1}{\mu} C^* + \frac{r_2}{\mu} T^* + \frac{r_3}{\mu} I^*, \quad (2.17)$$

$$I^* = \frac{(\alpha_1 C^* + \alpha_2 T^*)\Lambda - (\mu + \alpha_1 C^* + \alpha_2 T^*)((\mu + d_1 + r_1)C^* - (\mu + d_2 + r_2)T^*)}{(\mu + d_1 + d_2 + r_3)(\mu + \alpha_1 C^* + \alpha_2 T^*)}. \quad (2.18)$$

2.3.2 Reproduction number

The reproduction number, denoted as R_0 , tracks the new infections brought about by the introduction of one infectious individual into a susceptible population. The next generation matrix is used to find the reproduction number by considering the infectious classes (C, T, I) and classifying the new infections into \mathcal{F} and the negation of the outward transmission into \mathcal{V} , thus

$$\mathcal{F} = \begin{pmatrix} \alpha_1 SC \\ \alpha_2 ST \\ \beta_1 CT + \beta_2 CT \end{pmatrix}, \quad \mathcal{V} = \begin{pmatrix} \beta_1 CT + (\mu + d_1 + r_1)C \\ \beta_2 CT + (\mu + d_2 + r_2)T \\ (\mu + d_1 + d_2 + r_3)I \end{pmatrix}. \quad (2.19)$$

which implies that

$$(\nabla F)_{E_0} (\nabla V)_{E_0}^{-1} = \begin{pmatrix} \frac{\alpha_1 \Lambda}{\mu(\mu + d_1 + r_1)} & 0 & 0 \\ 0 & \frac{\alpha_2 \Lambda}{\mu(\mu + d_2 + r_2)} & 0 \\ 0 & 0 & 0 \end{pmatrix}. \quad (2.20)$$

The eigenvalues of $(\nabla F)_{E_0} (\nabla V)_{E_0}^{-1}$ are found from the equation

$$\begin{vmatrix} \frac{\alpha_1 \Lambda}{\mu(\mu + d_1 + r_1)} - \lambda & 0 & 0 \\ 0 & \frac{\alpha_2 \Lambda}{\mu(\mu + d_2 + r_2)} - \lambda & 0 \\ 0 & 0 & -\lambda \end{vmatrix} = 0$$

as

$$\lambda_1 = \frac{\alpha_1 \Lambda}{\mu(\mu + d_1 + r_1)}, \quad \lambda_2 = \frac{\alpha_2 \Lambda}{\mu(\mu + d_2 + r_2)}, \quad \lambda_3 = 0 \quad (2.21)$$

Finally, the basic reproduction number is

$$R_0 = \max\{\lambda_1, \lambda_2, \lambda_3\} = \max\left\{\frac{\alpha_1 \Lambda}{\mu(\mu + d_1 + r_1)}, \frac{\alpha_2 \Lambda}{\mu(\mu + d_2 + r_2)}, 0\right\}. \quad (2.22)$$

Theorem 2.1

The DFE is locally asymptotically stable if $R_0 < 1$.

Proof.

The Jacobian matrix for the system (2.1 – 2.5) is

$$J = \begin{pmatrix} -(\mu + \alpha_1 C + \alpha_2 T) & -\alpha_1 C & -\alpha_2 S & 0 & 0 \\ \alpha_1 C & \alpha_1 S - \beta_1 T - (\mu + d_1 + r_1) & -\beta_1 C & 0 & 0 \\ \alpha_2 T & -\beta_2 T & \alpha_2 S - \beta_2 T - (\mu + d_2 + r_2) & 0 & 0 \\ 0 & \beta_1 T + \beta_2 T & \beta_1 C + \beta_2 C & -(\mu + d_1 + d_2 + r_3) & 0 \\ 0 & r_1 & r_2 & r_3 & -\mu \end{pmatrix}.$$

When we substitute the DFE, we get

$$J = \begin{pmatrix} -\mu & 0 & -\alpha_2 \frac{\Lambda}{\mu} & 0 & 0 \\ 0 & \frac{\alpha_1 \Lambda}{\mu} - (\mu + d_1 + r_1) & 0 & 0 & 0 \\ 0 & 0 & \frac{\alpha_2 \Lambda}{\mu} - (\mu + d_2 + r_2) & 0 & 0 \\ 0 & 0 & 0 & -(\mu + d_1 + d_2 + r_3) & 0 \\ 0 & r_1 & r_2 & r_3 & -\mu \end{pmatrix}.$$

The characteristic equation therefore gives

$$\begin{vmatrix} -\mu - \lambda & 0 & -\alpha_2 \frac{\Lambda}{\mu} & 0 & 0 \\ 0 & \frac{\alpha_1 \Lambda}{\mu} - (\mu + d_1 + r_1) - \lambda & 0 & 0 & 0 \\ 0 & 0 & \frac{\alpha_2 \Lambda}{\mu} - (\mu + d_2 + r_2) - \lambda & 0 & 0 \\ 0 & 0 & 0 & -(\mu + d_1 + d_2 + r_3) - \lambda & 0 \\ 0 & r_1 & r_2 & r_3 & -\mu - \lambda \end{vmatrix} = 0.$$

Taking the determinant along the last row and last column, we have

$$\lambda \begin{vmatrix} -\mu - \lambda & 0 & -\alpha_2 \frac{\Lambda}{\mu} & 0 \\ 0 & \frac{\alpha_1 \Lambda}{\mu} - (\mu + d_1 + r_1) - \lambda & 0 & 0 \\ 0 & 0 & \frac{\alpha_2 \Lambda}{\mu} - (\mu + d_2 + r_2) - \lambda & 0 \\ 0 & 0 & 0 & -(\mu + d_1 + d_2 + r_3) - \lambda \end{vmatrix} = 0.$$

Again, taking the determinant along the last row and last column, we have

$$\lambda \begin{vmatrix} -\mu - \lambda & 0 & -\alpha_2 \frac{\Lambda}{\mu} \\ 0 & \frac{\alpha_1 \Lambda}{\mu} - (\mu + d_1 + r_1) - \lambda & 0 \\ 0 & 0 & \frac{\alpha_2 \Lambda}{\mu} - (\mu + d_2 + r_2) - \lambda \end{vmatrix} = 0$$

Taking the determinant along the last row and last column one more time, we have

$$\lambda \begin{vmatrix} -\mu - \lambda & 0 \\ 0 & \frac{\alpha_1 \Lambda}{\mu} - (\mu + d_1 + r_1) - \lambda \end{vmatrix} = 0$$

and finally

$$(-\mu - \lambda)(-\mu - \lambda)(-\mu + d_1 + d_2 + r_3) - \lambda \left(\frac{\alpha_2 \Lambda}{\mu} - (\mu + d_2 + r_2) - \lambda \right) \left(\frac{\alpha_1 \Lambda}{\mu} - (\mu + d_1 + r_1) - \lambda \right) (-\mu - \lambda) = 0$$

which means

$$\lambda_1 = -\mu, \lambda_2 = -(\mu + d_1 + d_2 + r_3), \lambda_3 = \frac{\alpha_2 \Lambda}{\mu} - (\mu + d_2 + r_2), \lambda_4 = \frac{\alpha_1 \Lambda}{\mu} - (\mu + d_1 + r_1), \lambda_5 = -\mu.$$

All eigenvalues are negative only if

$$\begin{aligned} \text{for } \lambda_3 < 0, \quad \text{we require } \frac{\alpha_2 \Lambda}{\mu} - (\mu + d_2 + r_2) < 0 &\Rightarrow \frac{\alpha_2 \Lambda}{\mu} < (\mu + d_2 + r_2) \Rightarrow \frac{\alpha_2 \Lambda}{\mu(\mu + d_2 + r_2)} < 1, \\ \text{for } \lambda_4 < 0, \quad \text{we require } \frac{\alpha_1 \Lambda}{\mu} - (\mu + d_1 + r_1) < 0, &\Rightarrow \frac{\alpha_1 \Lambda}{\mu} < (\mu + d_1 + r_1) \Rightarrow \frac{\alpha_1 \Lambda}{\mu(\mu + d_1 + r_1)} < 1 \Rightarrow R_0 < 1. \end{aligned}$$

3 Model Solution

The numerical method adopted in solving the model is the Runge-Kutta method (Oke, 2017). Given a system of differential equations

$$\dot{\mathbf{X}} = \mathbf{G}(t, \mathbf{X})$$

for some vector variable X , the Runge-Kutta scheme of the order 4 is as follows ;

$$\begin{aligned} \mathbf{K}_1 &= h\mathbf{G}(t, \mathbf{X}_n), & \mathbf{K}_2 &= h\mathbf{G}\left(t + \frac{h}{2}, \mathbf{X}_n + \frac{1}{2}\mathbf{K}_1\right), & \mathbf{K}_3 &= h\mathbf{G}\left(t + \frac{h}{2}, \mathbf{X}_n + \frac{1}{2}\mathbf{K}_2\right), & \mathbf{K}_4 \\ & & &= h\mathbf{G}(t + h, \mathbf{X}_n + \mathbf{K}_3) \end{aligned}$$

and the updated solution at the next time step $n + 1$ is

$$\mathbf{X}_{n+1} = \mathbf{X}_n + \frac{1}{6}(\mathbf{K}_1 + 2\mathbf{K}_2 + 2\mathbf{K}_3 + \mathbf{K}_4).$$

The model (2.1 - 2.5) is autonomous equation since the right hand side of all equations are not explicitly dependent on time and the Runge-Kutta scheme becomes

$$\mathbf{K}_1 = h\mathbf{G}(\mathbf{X}_n), \quad \mathbf{K}_2 = h\mathbf{G}\left(\mathbf{X}_n + \frac{1}{2}\mathbf{K}_1\right), \quad \mathbf{K}_3 = h\mathbf{G}\left(\mathbf{X}_n + \frac{1}{2}\mathbf{K}_2\right), \quad \mathbf{K}_4 = h\mathbf{G}(\mathbf{X}_n + \mathbf{K}_3)$$

with

$$\mathbf{X}_{n+1} = \mathbf{X}_n + \frac{1}{6}(\mathbf{K}_1 + 2\mathbf{K}_2 + 2\mathbf{K}_3 + \mathbf{K}_4),$$

where

$$\mathbf{X}_n = \begin{pmatrix} S_n \\ C_n \\ T_n \\ I_n \\ R_n \end{pmatrix}, \quad \mathbf{G}(\mathbf{X}_n) = \begin{pmatrix} \Lambda - \mu S_n - \alpha_1 S_n C_n - \alpha_2 S_n T_n \\ \alpha_1 S_n C_n - \beta_1 C_n T_n - (\mu + d_1) C_n - r_1 C_n \\ \alpha_2 S_n T_n - \beta_2 C_n T_n - (\mu + d_2) T_n - r_2 T_n \\ \beta_1 C_n T_n + \beta_2 C_n T_n - (\mu + d_1 + d_2) I_n - r_3 I_n \\ r_1 C_n + r_2 T_n + r_3 I_n - \mu R_n \end{pmatrix}$$

It is worth noting that there are 11 parameters whose values are obtained from literature or by estimation. The parameters pertaining to tuberculosis and its spread can be found in Das *et al.* (2021) and while the parameters

pertaining to the spread of COVID-19 can be found in Oke *et al.* (2021). The choices of the parameter values are as follows;

$$\Lambda = 0.0001; \mu = 0.0012; \alpha_1 = 0.000085044; \alpha_2 = 0.4048; \beta_1 = 0.01; \beta_2 = 0.01; \\ d_1 = 2.51357e - 6; d_2 = 2.51357e - 6; r_1 = 0.000334287; r_2 = 0.104; r_3 = 0.01.$$

By varying the values of the parameters, the model is solved and the outcomes are graphed for visualisation. The validation of the the findings from the qualitative analysis are shown in Figures (3.2a) and (3.2b) where the behaviours of the different sub-populations are illustrated.

3.1.1 Validation of Solution

For the sake of validation, the solutions are considered for two cases where $R_0 < 1$ and $R_0 > 1$. From Figures (3.2a), it is clear that the system is stable for $R_0 < 1$ and Figure (3.2b) shows that the system is unstable for $R_0 > 1$. This validates the quantitative analysis and the numerical approach can therefore be used to find the solution as we vary the values of the parameters.

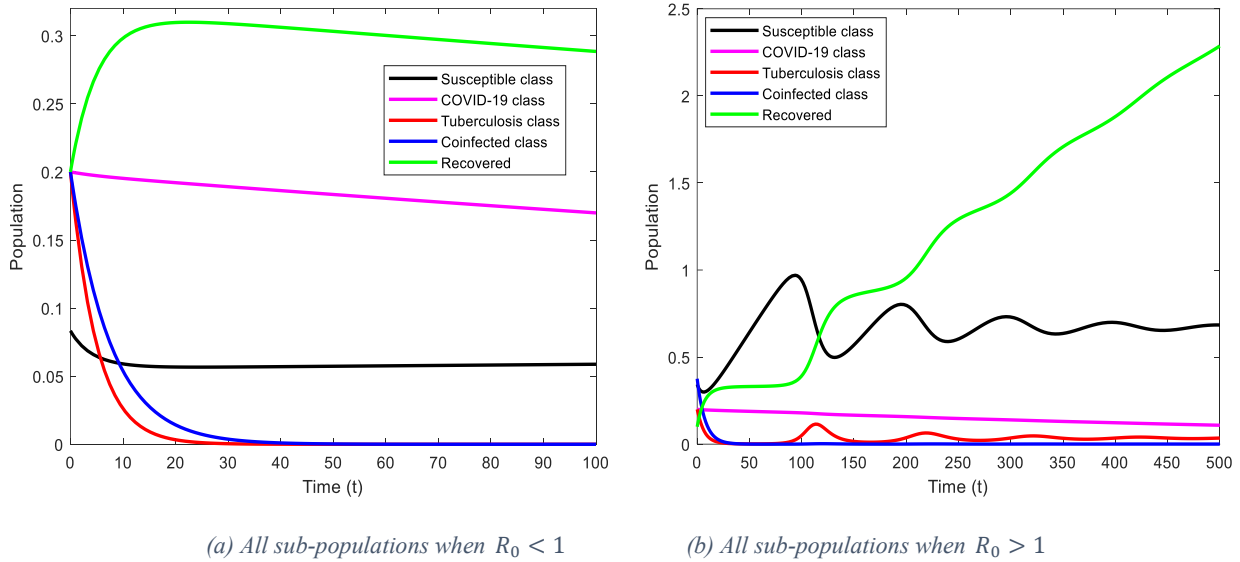


Figure 3.1: Verifying the stability of the equilibrium points

4 Discussion of Results

The aim of this study is to investigate the trend of co-infection of COVID-19 and tuberculosis in a population. The pertinent parameters are varied and the impact on the dynamics of both diseases are studied.

The rate at which the susceptible sub-population gets infected with COVID-19 is denoted as α_1 and the rate at which susceptible sub-population gets infected with tuberculosis is denoted as α_2 . The rates are varied to investigate their effects on the five sub-populations and the outcomes are shown in Figures (4.1 – 4.5). As shown in Figure (4.1), increasing the rate at which individuals get infected with one disease will lead to extinction of the susceptible sub-population. The consequence of increasing α_1 and α_2 is a rapid removal from the susceptible class and thus, reduction in the susceptible class is expected. However, comparing Figures (4.1a) and (4.1b) shows that the effect of increasing rate of contracting tuberculosis is more significant than the effect of increasing rate of contracting COVID-19. Figure (4.2) illustrate the dynamics of the COVID-19 sub-population as the rate of contracting only COVID-19 and the rate of contracting only tuberculosis are varied. The COVID-19 sub-population continues to rise as the rate of

contracting only COVID-19 increases while the COVID-19 sub-population reduces as the rate of contracting only tuberculosis increases. By comparing Figures (4.2a) and (4.2b), it can be seen that rates of increase in the COVID-19 sub-population as α_1 increases is higher than the rate at which COVID-19 sub-population decreases with increasing α_2 . Figure (4.3) shows that as the rate of single infection increases, the tuberculosis sub-population experiences an initial increase before the trend changes downward until there are no tuberculosis subpopulation any more. Figure (4.3a) depicts the response of the tuberculosis sub-population to an increase in the rate (α_1) of contracting COVID-19 only. The maximum population of the tuberculosis sub-population is obtained at the lowest α_1 and the peak of the COVID-19 subpopulation reduces with increasing α_1 . Meanwhile, Figure (4.3b) shows that the response of the tuberculosis sub-population to an increase in the rate (α_2) of contracting tuberculosis only. The maximum population of the tuberculosis sub-population is obtained at the highest α_2 and the peak of the tuberculosis sub-population increases with increasing α_1 . As the rate at which susceptible sub-population get infected with only one disease increases, the co-infected sub-population increases. The increase is more pronounced when the rate of infection with tuberculosis only increases. Figure (4.4a) and (4.4b) show that the coinfectd population increases with increasing rate of recruitment into any diseased subpopulation. The recovered sub-population is shown in figure (4.5a) to reduce as the rate of getting COVID-19 only increases and figure (4.5b) shows that the recovered sub-population increases when the rate of getting tuberculosis only increases.

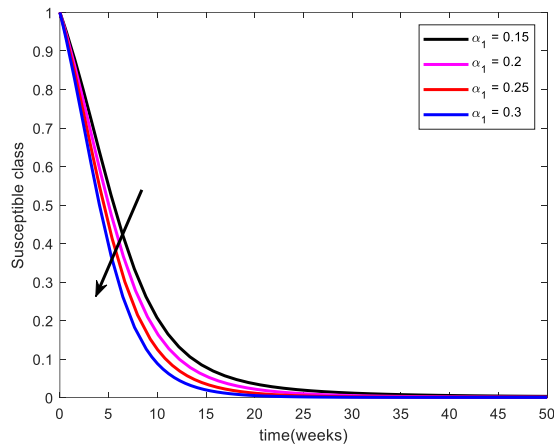
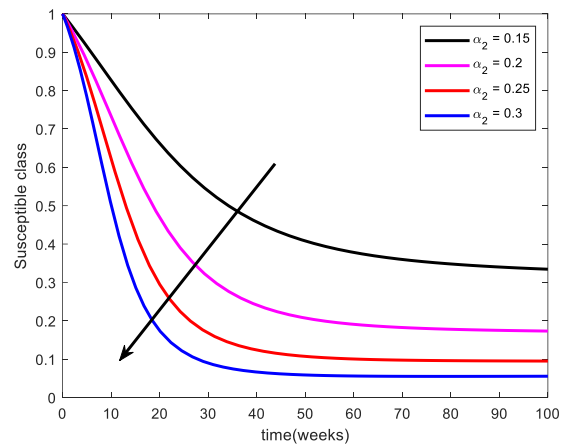
(a) Susceptible class with α_1 (b) Susceptible class with α_2

Figure 4.1: Susceptible class with rates of single infection

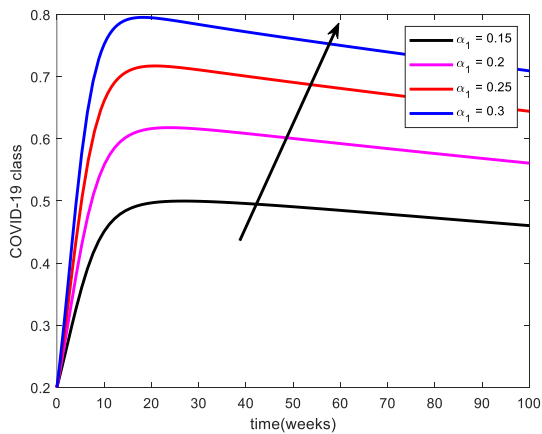
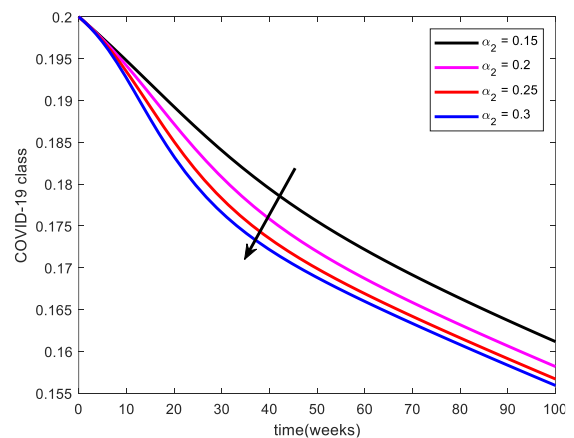
(a) COVID-19 class with α_1 (b) COVID-19 class with α_2

Figure 4.2: COVID-19 class with rates of single infection

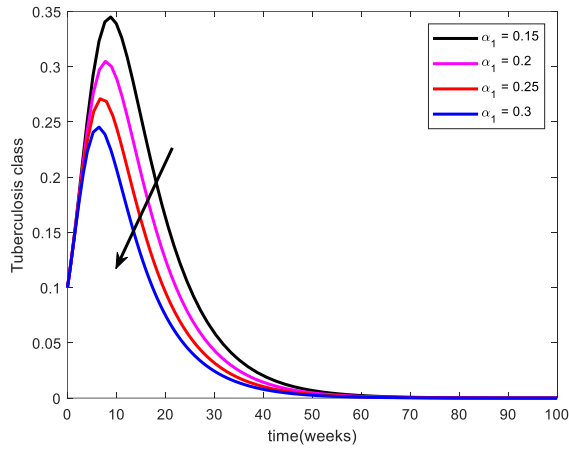
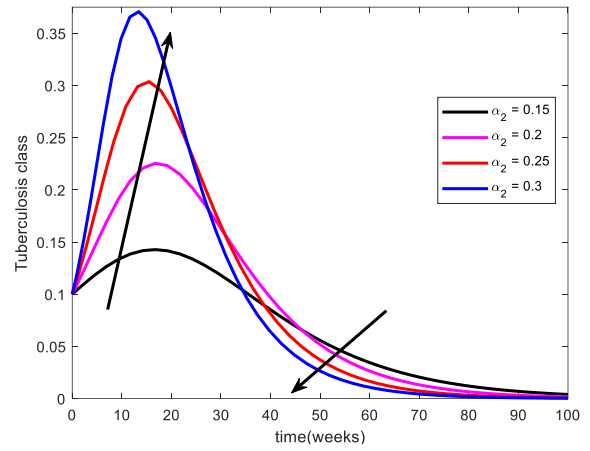
(a) Tuberculosis class with α_1 (b) Tuberculosis class with α_2

Figure 4.3: Tuberculosis class with rates of single infection

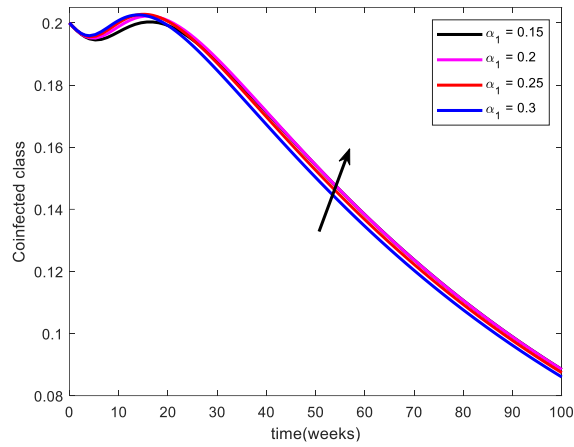
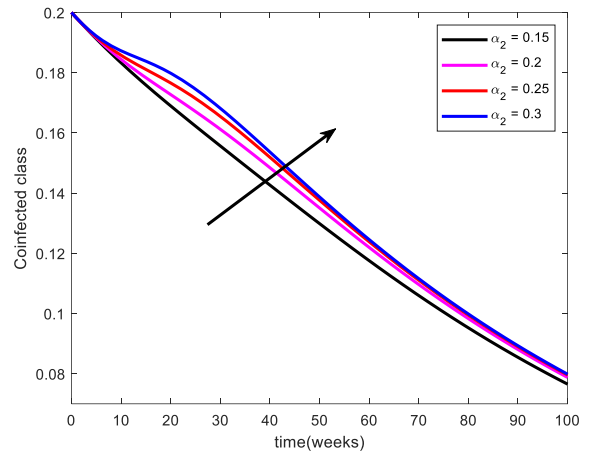
(a) Co-infected class with α_1 (b) Co-infected class with α_2

Figure 4.4: Co-infected class with rates of single infection

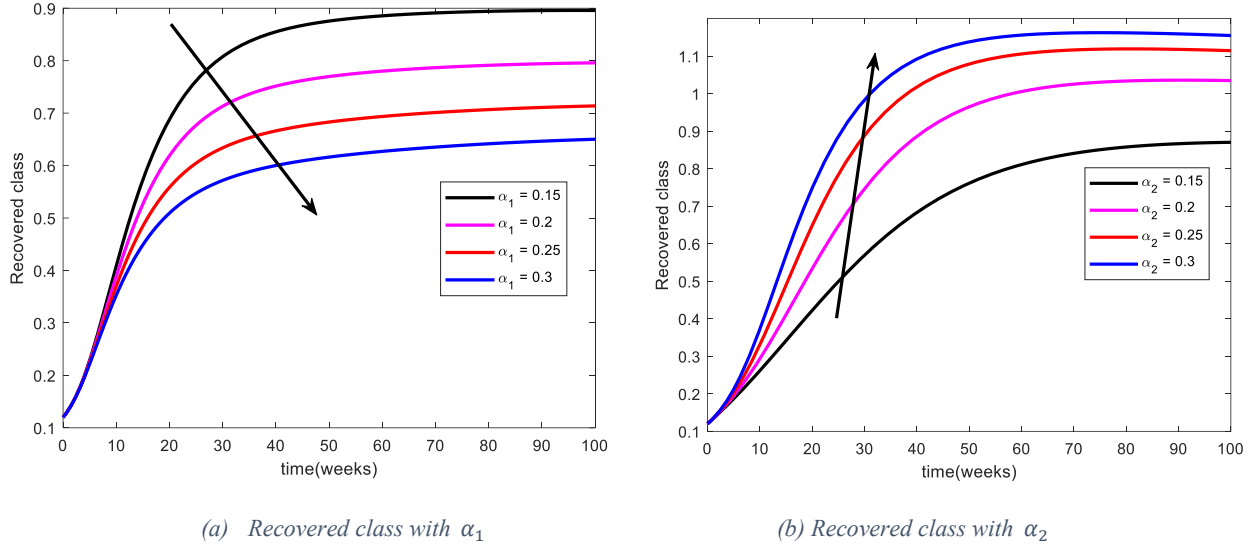


Figure 4.5: Recovered class with rates of single infection

5 Conclusion

This study investigates a population where individuals can be coinfecting with COVID-19 and tuberculosis. A deterministic mathematical model is formulated to explain the trend in the co-infection of COVID-19 and tuberculosis in a population. The equilibria for the governing equations were obtained as

$$E_0 = \left(\frac{\Lambda}{\mu}, 0, 0, 0 \right) \text{ and } (S^*, E^*, C^*, T^*, I^*, R^*)$$

where

$$S^* = \frac{\Lambda}{\mu + \alpha_1 C^* + \alpha_2 T^*}, \quad R^* = \frac{r_1}{\mu} C^* + \frac{r_2}{\mu} T^* + \frac{r_3}{\mu} I^*,$$

$$I^* = \frac{(\alpha_1 C^* + \alpha_2 T^*) \Lambda - (\mu + \alpha_1 C^* + \alpha_2 T^*) ((\mu + d_1 + r_1) C^* - (\mu + d_2 + r_2) T^*)}{(\mu + d_1 + d_2 + r_3)(\mu + \alpha_1 C^* + \alpha_2 T^*)}.$$

The reproduction number is also calculated to track the number of possible new infections and we obtain the reproduction number as

$$R_0 = \max \left\{ \frac{\alpha_1 \Lambda}{\mu(\mu + d_1 + r_1)}, \frac{\alpha_2 \Lambda}{\mu(\mu + d_2 + r_2)}, 0 \right\}.$$

The disease-free equilibrium point is found to be locally asymptotically stable if $R_0 < 1$. The non-negativity condition for the model was established and the Runge-Kutta method of order 4 was used to solve the model. The model is simulated for various parameter values and the following outcomes are observed;

- (i) Increasing the rate at which individuals get infection with a single disease (either COVID-19 or tuberculosis) poses the risk of coinfecting every member of the population. Also, it is found that the rate of contracting tuberculosis poses more significant effect on the possibility of coinfection than COVID-19.

- (ii) The maximum tuberculosis sub-population is obtained at the lowest rate of recruitment into the COVID-19 subpopulation while the maximum COVID-19 sub-population is obtained at the highest rate of recruitment into the COVID-19 subpopulation.
- (iii) Migrations from COVID-19 to co-infected sub-population or from tuberculosis to co-infected sub-population both result in an increase in the co-infected population. The effects of migration from tuberculosis sub-population is more significant than migration from COVID-19.

Based on the results obtained from this project, the below are the recommendations made;

- (i) Since the rate of contracting tuberculosis poses more significant effect on the possibility of coinfection than COVID-19, caution has to be placed to ensure that COVID-19 is not allowed to thrive in the population where tuberculosis is rampant.
- (ii) Stringent measures (such as the use of nose mask, travel restrictions, handwashing, periodic sanitisers, and social distancing) are necessary to prevent the tuberculosis from reaching the maximum. These measures are able to reduce recruitment into the COVID-19 subpopulation.

References

- Aldila, D., Khoshnaw, S. H. A., Safitri, E., Anwar, Y. R., Bakry, A. R. Q., Samiadji, B. M., Amugerah, D. A., Farhan, M., Ayulani, I. D., and Salim, S. N. (2020). A mathematical study on the spread of COVID-19 considering social distancing and rapid assessment: The case of Jakarta, Indonesia. *Chaos, Solitons & Fractals*, page 110042.
- Annas, S., Isbar Pratama, M., Rifandi, M., Sanusi, W., and Side, S. (2020). Stability Analysis and Numerical Simulation of SEIR Model for pandemic COVID-19 spread in Indonesia. *Chaos, Solitons & Fractals*, page 110072.
- Ayinla, A. Y., Othman, W. A. M., and Rabi, M. (2021). A Mathematical Model of the Tuberculosis Epidemic. *Acta Biotheoretica*, 69(3):225–255.
- Bada, O. I., Oke, A. S., Mutuku, W. N., and Aye, P. O. (2021). Analysis of the Dynamics of SI-SI-SEIR Avian Influenza A(H7N9) Epidemic Model with Reinfection. *Earthline Journal of Mathematical Sciences*, 5(1):43–73.
- Bada, O. I., Oke, A. S., Mutuku, W. N., & Aye, P. O. (2021). Analysis of the dynamics of SI-SI-SEIR Avian influenza A (H7N9) epidemic model with re-infection. *Earthline Journal of Mathematical Sciences*, 5(1), 43-73.
- Bates, J. H. and Stead, W. W. (1993). The history of tuberculosis as a global epidemic. *Medical Clinics of North America*, 77(6):1205–1217.
- CDC (2020). Covid-19 dashboard.
- Chong, K. C., Leung, C. C., Yew, W. W., Zee, B. C. Y., Tam, G. C. H., Wang, M. H., Jia, K. M., Chung, P. H., Lau, S. Y. F., Han, X., and Yeoh, E. K. (2019). Mathematical modelling of the impact of treating latent tuberculosis infection in the elderly in a city with intermediate tuberculosis burden. *Scientific Reports*, 9(1).
- Das, K., Murthy, B. S. N., Samad, S. A., and Biswas, M. H. A. (2021). Mathematical transmission analysis of SEIR tuberculosis disease model. *Sensors International*, 2:100120.
- Fatmawati, Khan, M. A., Bonyah, E., Hammouch, Z., and Shaiful, E. M. (2020). A mathematical model of tuberculosis (TB) transmission with children and adults groups: A fractional model. *AIMS Mathematics*, 5(4):2813–2842.
- Horowitz, R. I. and Freeman, P. R. (2020). Three novel prevention, diagnostic, and treatment options for COVID-19 urgently necessitating controlled randomized trials. *Medical Hypotheses*, 143:109851.
- Kabunga, S. K., Goufo, E. F. D., and Tuong, V. H. (2020). Analysis and simulation of a mathematical model of tuberculosis transmission in Democratic Republic of the Congo. *Advances in Difference Equations*, 2020(1).
- Kimulu A. M., Oke A. S., & Ndambuki, M. C. (2023). Mathematical Model for HIV-COVID-19 Co-Infection Dynamics in Kenya. *International Journal of Innovative Science and Research Technology*, 8(8), 767 - 777
- Kimulu, A. M., Mutuku, W. N., Mwalili, S. M., Malonza, D., & Oke, A. S. (2022a). Male Circumcision: A Means to Reduce HIV Transmission between Truckers and Female Sex Workers in Kenya. *Journal of Mathematical Analysis and Modeling*, 3(1), 50-59.

- Kimulu, A. M., Mutuku, W. N., Mwalili, S. M., Malonza, D., & Oke, A. S. (2022b). Mathematical Modelling of the Effects Funding on HIV Dynamics Among Truckers and Female Sex Workers Along the Kenyan Northern Corridor Highway.
- Kumar Raghav, P. and Mohanty, S. (2020). Are graphene and graphene-derived products capable of preventing COVID-19 infection? *Medical Hypotheses*, 144:110031.
- Li, T., Zhang, T., Gu, Y., Li, S., and Xia, N. (2021). Current progress and challenges in the design and development of a successful COVID-19 vaccine. *Fundamental Research*, 1(2):139–150.
- Mekonen, K. G., Balcha, S. F., Obsu, L. L., and Hassen, A. (2022). Mathematical Modeling and Analysis of TB and COVID-19 Coinfection. *Journal of Applied Mathematics*, 2022:1–20.
- Nainggolan, J., Supian, S., Supriatna, A. K., and Anggriani, N. (2013). Mathematical model of tuberculosis transmission with recurrent infection and vaccination. *Journal of Physics: Conference Series*, 423:012059.
- Ndendya, J. Z., Mlay, G., & Rwezaura, H. (2024). Mathematical modelling of COVID-19 transmission with optimal control and cost-effectiveness analysis. *Computer Methods and Programs in Biomedicine Update*, 5, 100155.
- Oke, A. S. (2017). Convergence of differential transform method for ordinary differential equations. *Journal of Advances in Mathematics and Computer Science*, 24(6), 1-17.
- Oke A. S., & Bada, O. I. (2019). Analysis of the dynamics of avian influenza A (H7N9) epidemic model with re-infection. *Open Journal of Mathematical Sciences*, 3(1), 417.
- Oke, A. S., Bada, O. I., Rasaq, G., and Adodo, V. (2021). Mathematical analysis of the dynamics of COVID-19 in Africa under the influence of asymptomatic cases and re-infection. *Mathematical Methods in the Applied Sciences*.
- Okuonghae, D. and Ikhimwin, B. O. (2016). Dynamics of a mathematical model for tuberculosis with variability in susceptibility and disease progressions due to difference in awareness level. *Frontiers in Microbiology*, 6.
- Okundalaye, O. O., Othman, W. A. M., & Oke, A. S. (2022). Toward an efficient approximate analytical solution for 4-compartment COVID-19 fractional mathematical model. *Journal of computational and applied mathematics*, 416, 114506.
- Oswald, S., Liana, Y., Mlay, G., & Kidima, W. B. (2024). Modelling Optimal Control of Bovine Tuberculosis Transmission Dynamics with Associated Costs Public Health Education Campaign, Treatment and Vaccination Cost Effective?. Available at SSRN 4688591.
- Paul, S., Mahata, A., Ghosh, U., & Roy, B. (2021). Study of SEIR epidemic model and scenario analysis of COVID-19 pandemic. *Ecological Genetics and Genomics*, 19, 100087.
- Paul, S., Mahata, A., Mukherjee, S., Mali, P. C., & Roy, B. (2023). Fractional order SEIQRD epidemic model of Covid-19: A case study of Italy. *PLoS One*, 18(3), e0278880.
- Paul, S., Mahata, A., Karak, M., Mukherjee, S., Biswas, S., & Roy, B. (2024). A fractal-fractional order Susceptible-Exposed-Infected-Recovered (SEIR) model with Caputo sense. *Healthcare Analytics*, 5, 100317.
- Seifirad, S. (2020). Pirfenidone: A novel hypothetical treatment for COVID-19. *Medical Hypotheses*, 144:110005.
- Toit, A. D. (2020). Outbreak of a novel coronavirus. *Nature Reviews Microbiology*, 18(3):123–123.
- Wangari, I. M., Sewe, S., Kimathi, G., Wainaina, M., Kitetu, V., and Kaluki, W. (2021). Mathematical Modelling of COVID-19 Transmission in Kenya: A Model with Reinfection Transmission Mechanism. *Computational and Mathematical Methods in Medicine*, 2021:1–18.
- Zafar, Z. U. A., Hussain, M. T., Inc, M., Baleanu, D., Almohsen, B., Oke, A. S., & Javeed, S. (2022). Fractional-order dynamics of human papillomavirus. *Results in Physics*, 34, 105281.
- Shaikh R, Porwal P, Gupta VK. An SEIRS Epidemic Model with Immigration and Vertical Transmission. Asian Res. J. Math. [Internet]. 2020 Dec. 19 [cited 2024 May 25];16(11):48-53. Available from: <https://journalarjom.com/index.php/ARJOM/article/view/383>
- El Hajji M. Optimal Control of an "SIR" Epidemic Model in a Chemostat Using Some Suitable Protein Doses. J. Adv. Math. Com. Sci. [Internet]. 2019 Feb. 25 [cited 2024 May 25];30(6):1-15. Available from: <https://journaljamcs.com/index.php/JAMCS/article/view/1327>
- Wei HM, Li XZ, Martcheva M. An epidemic model of a vector-borne disease with direct transmission and time delay. *Journal of Mathematical Analysis and Applications*. 2008 Jun 15;342(2):895-908.